UNCLASSIFIED

AD NUMBER
ADB013138

| LIMITATION CHANGES |

TO:

Approved for public release; distribution is unlimited.

FROM:

Distribution authorized to U.S. Gov't. agencies only; Test and Evaluation; JUL 1976. Other requests shall be referred to U.S. Army Ballistic Research Laboratories, Aberdeen Proving Ground, MD, 21005.

| AUTHORITY |

BRL ltr, 8 Mar 1978

THIS PAGE IS UNCLASSIFIED

AD

BRL

REPORT NO. 1899

PLANE SHOCK - THERMAL LAYER INTERACTIONS

E. J. Gion

July 1976

USA BALLISTIC RESEARCH LABORATORIES
ABERDEEN PROVING GROUND, MARYLAND 21005

attn. DRXBR-TS-

REPORT DOCUMENTATION PAGE	READ INSTRUCTIONS BEFORE COMPLETING FORM

1. REPORT NUMBER	2. GOVT ACCESSION NO.	3. RECIPIENT'S CATALOG NUMBER
BRL 1899		

4. TITLE (and Subtitle)	5. TYPE OF REPORT & PERIOD COVERED
PLANE SHOCK - THERMAL LAYER INTERACTIONS	Final rept.
	6. PERFORMING ORG. REPORT NUMBER

7. AUTHOR(s)	8. CONTRACT OR GRANT NUMBER(s)
E. J. Gion	

9. PERFORMING ORGANIZATION NAME AND ADDRESS	10. PROGRAM ELEMENT, PROJECT, TASK AREA & WORK UNIT NUMBERS
USA Ballistic Research Laboratories Aberdeen Proving Ground, Maryland 21005	1W161102AH43

11. CONTROLLING OFFICE NAME AND ADDRESS	12. REPORT DATE
U.S. Army Materiel Development and Readiness Command 5001 Eisenhower Avenue, Alexandria, VA 22333	JUL 1976
	13. NUMBER OF PAGES
	43

14. MONITORING AGENCY NAME & ADDRESS(if different from Controlling Office)	15. SECURITY CLASS. (of this report)
DA-1-W-161102-AH-43	UNCLASSIFIED
	15a. DECLASSIFICATION/DOWNGRADING SCHEDULE

16. DISTRIBUTION STATEMENT (of this Report)

17. DISTRIBUTION STATEMENT (of the abstract entered in Block 20, if different from Report)

18. SUPPLEMENTARY NOTES

19. KEY WORDS (Continue on reverse side if necessary and identify by block number)

Thermal Layers
Non-Ideal Blast Waves

Shock Interactions
Shock - Thermal Layer Interaction

— APPROXIMATELY

20. ABSTRACT (Continue on reverse side if necessary and identify by block number) (ner)

A model of the precursor phenomena produced by interaction of a plane shock wave with a heated air layer has been studied in the laboratory. Mostly a single shock Mach number of 1.11 was used for thermal layer temperatures between $\sim$ 500 - 1000°K. Interferometric observation provided temperatures in the thermal layer regions in front of and behind the shock. In the experiments, a new picture of the interaction process was obtained, resembling an "inverse" to the coalescence of Mach waves to a shock. With a few assumptions temperatures have been assigned to this "transition" region.

DD FORM 1 JAN 73 1473 EDITION OF 1 NOV 65 IS OBSOLETE

TABLE OF CONTENTS

LIST OF ILLUSTRATIONS

I. INTRODUCTION

Observation of so-called "precursor" shocks occurred early- more than two decades ago- in nuclear testing programs. In-the-field measurements for air bursts over terrain produced characteristic pressure traces which portray (see Figure 1) a significant pressure rise leading the main pressure wave arrival.[1] The importance of the precursor phenomenon for nuclear weapons lies in its alteration of the blast intensity and wave form: the dynamic pressure is signifi- cantly increased, thereby increasing the chances for defeat of struc- tures strengthened against static pressure forces but still vulnerable to drag forces.

The mechanism inducing the precursor formation in the field is generally believed to be the presence prior to shock arrival of a thermal layer adjacent to the earth's surface. Such a layer may be formed by irradiation of the earth's surface by the nuclear burst and subsequent evaporation of the surface into the adjoining air layer. This heated-air layer, the "thermal layer" so-called, carries with it a higher sound speed, with the important result that waves incident on and in the layer may travel faster in it and thus lead the portion of incident wave traveling in the colder region, thereby giving rise to the precursor.

Field measurements of the air temperature prior to shock arrival from the nuclear burst indicate rather high temperatures, $T \gtrsim 1200^\circ K$

having been recorded within a few feet of ground at ground ranges $GR \sim 300- 600m$.[2] The temperature history as well as its variation with height is less clearly known from these experiments, due to difficulties with instrumentation in the extreme environment and with interpretation of records.[3]

---

1. K. Kaplan, P. J. Norris, P. A. Ellis, and D. C. Sachs, "Nuclear Blast Phenomena - Vol. II." DASA 1200 (1971). CONFIDENTIAL. This reference contains an extensive bibliography and discussion of theoretical and experimental work on the precursor.

2. T. R. Broida, A. Broido, and A. B. Willoughby, "Air Temperature in the Vicinity of a Nuclear Detonation" Operation TUMBLER Project 8.2WT542.

3. E.C.Y. Inn, "Air Temperature Measurements Over Several Surfaces." Operation TEAPOT Project 8.4e WT-1149 (1957).

In the laboratory at about same time period the precursor phenomenon was studied by Griffith[4] and by Varwig and Zemel[5] using plane or reflected shocks interacting with air over a heated plate. Interesting features of the interaction are given, and Griffith makes comparisons with his theoretical model derived for moderate strength shocks and plate temperatures. Jahn[6] investigated the interaction of a plane shock incident on two gases of different sound speed separated by an interface. Discussion of significant features is based on detailed knowledge of gasdynamics and is invaluable in this respect.

Early theoretical treatments of a small disturbance incident on the interface between super- and subsonic regions and subsequent propagation of the disturbance have been made by Howarth[7] and by Tsien and Finston[8], whose interests then were pointed toward shock-boundary layer interactions. The principal finding appears to be that the disturbance in the subsonic region propagates upstream and ahead of that in the supersonic region. No detailed treatments exist insofar as is known for shocks or large disturbances analogous to the linearized treatments mentioned above. Simple phenomenological models[1] of idealized shock-thermal layer interaction have been constructed and analyzed in accordance with acoustical theory as well as with oblique shock theory. A major prediction, verified by laboratory experiments, is a relation between the precursor shock angle and temperature ratio of (uniform) hot and cold regions:

$$\sin p = (T_c/T_h)^{1/2}$$

Also, numerical techniques and models for predicting flows of great

4. W. C. Griffith, "Interaction of a Shock Wave with a Thermal Boundary Layer." J. Aero. Sci. 23, 16-23 (1956).

5. R. Varwig and J. Zemel, "The Interaction of Shock Waves with a Thermal Layer" NAVORD Report 4021, AFSWR 266 (1955).

6. R. G. Jahn, "The Refraction of Shock Waves at a Gaseous Interface - III. Irregular Refraction." Princeton University Tech. Report II19 (1955).

7. L. Howarth, "The Propagation of Steady Disturbances in a Supersonic Stream Bounded on One Side by a Parallel Subsonic Stream." Proc. Combr. Phil. Soc. 44, 380-90 (1948).

8. H. S. Tsien and M. Finston, "Interaction Between Parallel Streams of Subsonic and Supersonic Velocities." J. Aero. Sci. 16, 515-528 (1949).

complexity have been and are being developed.

The purpose of this work was to produce a clean-gas, model thermal layer with precisely known conditions and to study the interaction of a plane shock with the thermal layer. Observation by means of a Mach-Zehnder interferometer would allow deducing temperature profiles existing in the pre-shock and post-shock regions of the flow. Results would be useful for guidance and comparison with numerical models and predictions. The layer was created by a heated plate set in the test section of a shock tube, the same technique as used by Griffith[4] at much lower temperatures. A single shock condition was most thoroughly investigated, for a range of plate temperatures, although results at one or two other conditions were obtained. Results for shocks of small but realistic overpressures $(2.8-21)10^4$ Pa (4-30 psi) were thought desirable, with thermal layer temperatures of $\lesssim 1000^{\circ}$K. An accompanying objective during this project was to establish feasibility for methods of obtaining a thermal layer which would allow scaling up to a much larger area thermal layer over which a small explosive could be detonated, the rationale here being that the computer codes existing could model explosives and hence a more severe test of codes would be afforded.

II. EXPERIMENTAL APPARATUS AND PROCEDURES

A. Shock Generation and Conditions

As mentioned above, a plane shock generated in a shock tube interacts with a thermal layer created by a heated plate mounted in the test section. An over-all sketch of the experimental setup is shown in the Figure 2. The desired shock overpressures were obtained approximately by use of driver-to-driven pressure ratios given by one-dimensional shock tube theory. The precise flow condition at the test section is then obtained from the monitored shock velocity by use of shock tube tables. Fast response, commercially available quartz piezoelectric pressure gages monitored the shock velocity; and measurements between gage oscilloscope traces are expected to give shock velocity to within ± 1%, as is usual in shock tube work.

B. Mach-Zehnder Interferometer

The Mach-Zehnder interferometer used in these experiments has 25 cm diameter plates recently resurfaced, to adequately image the fine fringes seen in the thermal layer. Backlighting for the interferometer was provided by a 2J passive-dye Q-switched ruby laser. Aside from apparent operation under Murphy's Laws*, the laser back-

---

*Murphy's propositions are, according to a f. n., p. 393, H. T. Davis, Introduction to Nonlinear Differential and Integral Equations: 1) If anything can go wrong, it will; 2) Things when left alone can only go from bad to worse; 3) Nature sides with the hidden flaw.

9

lighting provided ample intensity and a well defined wavelength for the data reduction procedures.

A problem with graininess in the film image was noted and caused some concern. A disc of ordinary sawn quartz had been in use[9] to diffuse and scatter adequately, thus to broaden and smooth out intensity variations in the small laser ($\lesssim$ 1 mm diam) beam before its entering the collimating lens. However, repeated firings at the high power densities had apparently caused deterioration of the special properties inherent in the particular area used of the quartz disc, resulting in objectionable film graininess. And efforts to find another suitable spot on this and other such discs were abandoned, when chances for success appeared minimal and not clearly repeatable.

An obvious beam broadener is the ordinary ground glass screen. However, observation in the film plane with a small cw laser shows merely that granularity associated with ground glass. But, motion of the glass in its plane (normal to optical axis) produces an acceptably evenly illuminated field, an observation noted several years earlier.[10] However, such motion and transport during pulsed operation are beyond present technology, and this sort of modification to the optical train was not entertained. Instead, it was hoped that an effect analogous to plate motion could be achieved by simply using two ground glass plates in the beam, with random granular structures of the two plates falling again randomly in the film plane, but now more evenly distributed. Happily such was the case, and the film plane was once again satisfactorily illuminated. Trials showed that other ground glass pairs could be thrust into the beam with no apparent loss in quality of illumination. A small, uncritical separation between plates was seemingly necessary to obtain optimum contrast. All of the pictures produced in this report were made with this simple beam broadener.

C. Heated Plate Thermal Layer

An important goal in this project was to devise a means of production of a regular, well-defined thermal layer. The technique chosen would lend itself as mentioned in the Introduction, to scaling upward for producing a similar layer of much larger extent for testing with explosives. A number of methods was considered: 1) flowing of a heated layer of air over test plate or test section wall; 2) rapid heating of the air above a plate via a grid of suddenly energized

9. F. H. Oertel, "Laser Interferometry of Unsteady Underexpanded Jets." BRL R 1694 (1974) AD 773664.

10. T. A. Wiggins, "Methods for Spreading Laser Beams." Appl. Optics 10, 963-5 (1971).

electrical wires or ribbon; 3) electrical resistance heating of a plate which then acts to heat the adjacent air at the testing station; 4) heating of a suitable plate via microwaves, possibly making use of surplus radar antennas (?); 5) burning of a layer of gaseous fuel. Because of experimental limitations the decision was made to proceed with 3), the brute-force method, on the thought that success was more assured both in producing the thermal layer at desired temperatures and in scaling upward to the larger thermal layers. Results of the homemade electrical furnace are shown in the Figure 3. Only construction-type fire brick (thermal conductivity $\sim$ 0.6 Btu/hr. ft.^{o}F) was used since on hand, and these were laid into top and bottom sections of the piece of 30 cm diameter aluminum pipe to form a heating cavity for the 41 X 10 X 1.25 cm steel test plate. Resistance wire was used to allow $\sim$ 1000 W heating rate as an initial trial. The commercial availability of much better insulating materials in both brick and wool blanket form (thermal conductivity $\sim$ 0.03 Btu/hr. ft.^{o}F) suggest much greater heating efficiencies are possible over the present crude assembly. Thus, scaling the furnace to larger sizes entails simply stringing of more lengths of resistance wire and blanketing with more insulating material.

A heating rate curve for the oven, as measured by a thermocouple located near a wall of the cavity with test plate in place, is shown in Figure 4a. The accompanying heating rate for the test plate, as measured by a thermocouple brazed to test plate's bottom surface, is also shown. A cooling curve for the test plate mounted in the test section is shown in Figure 4b. The thermocouple readings are expected to be merely indicative of the plate's test-surface temperatures since the plate is mounted in an inverted position near the top of the test section to reduce convection currents in the thermal layer. Occasional sanding and polishing of the test plate was done to remove scale, a possible source of hot spots.

D. Typical Run Sequence

For a typical run the following steps were usually taken: With oscilloscopes and monitoring instrumentation adequately warmed up, with test plate oven temperature in the desired range, the plate with sting attached is removed from the oven and (cold) mounting stud affixed to back surface. The plate assembly is then brought over and thrust into the test section and fastened to its ceiling and back end, while simultaneously, final adjustments for the laser Q-switching are made. The driver section then receives its final charge of dry N_2 for the selected pressure, with the driven section at atmospheric. Simultaneously, the film is opened in the darkened test section building, and recording and monitoring systems readied for the run. The shot is taken usually 1-1/2 - 3 minutes after opening of the oven.

E. Data Generation

Records from a typical run are shown in Figure 5. The shock
passage over successive gages is pictured in the oscilloscope traces
and permits setting of the delayed triggering of the laser to capture
the shock at the test section window. The interferogram for this run
is shown, and these records constitute the principal raw data of an
experiment.

A closer look at the interferogram reveals a number of interesting
features and suggests a picture of the interaction process. The un-
disturbed region and the uniform region behind the shock in the cold
air are characterized by the (more or less) straight fringes. The
very fine and closely spaced fringes "above" the heated plate characterize
the heated air layer. Last but not least is an interesting feature also
observed by Griffith[4] of shock-thermal layer interaction: one notes a
"transition" region, a rounding, shifting of fringes through the
shocked region as one goes from the base of the shock in the cold region
to the thermal layer. Some of our rounding fringes seem broken into
straight line segments and suggest that the primary shock degenerates
into a set of weak shocks or pressure waves traversing the "transition"
region near the thermal layer. In this run the plate (surface)
temperature was determined to be $705^{\circ}K$, with sound speed near the
plate much greater than shock speed in the cold air; thus the shock
does not penetrate to the plate surface. However, a weak disturbance
is to be noted throughout the height of the layer if one follows
individual fringes in the layer. The disturbance apparently is a
continuation into the layer of the leading portion of the foot of the
shock disturbance. The small fringe shifts noted in the layer
represent the flow property adjustment to either side of the disturbance.
A second interferogram, using the "infinite-fringe" setting, is shown
in the Figure 6. A number of runs were made using this setting because
of greater simplicity in reduction, although generally less accurate.
However, some features of the flow are exhibited more prominently
than in the regular multifringe setting of Figure 5. Particularly one
notices in the transition zone the fanning out of the fringes coming
down from the main shock. Since in the infinite fringe setting the
fringes represent contours of constant density, one has more explicitly
the picture mentioned above of the degeneration of the shock into a
set of waves.

F. Data Reduction

The (average) shock velocity at the test location is determined
as mentioned previously from the time interval between shock passage
over gage stations of known separation. In turn, all the properties
behind the shock are known in the ideal gas case, which is assumed
throughout the present work for the weak shocks and the thermal layer
temperatures involved.

12

Fringes in an interferogram are "read out" on a large screen digitizing comparator. The interferogram reduction requires the fringe shift measurement in the desired region of flow plus presumably known initial conditions of the cold air. The fringe shift equation relates the fringe shift to the density change through the Gladstone-Dale relation and may be written

$$\delta = \beta \; (L/\lambda) \; (\frac{\rho_b - \rho_a}{\rho_s})$$

where

δ = fringe shift from undisturbed fringe (spacing)

β = (a constant for the gas related to the refractivity K) = $K\rho_s$

L = geometric path through the disturbance

λ = wavelength of source light

ρ_b, ρ_a, ρ_s = densities; ρ_b is density producing the fringe shift δ from initial density ρ_a, with ρ_s the standard density at 273.2°K and 1.01325 x 10^5 Pa

Use of the ideal gas equation of state $p = \rho RT/M$ leads to an expression for temperature T in terms of the fringe shift

$$T_s/T_b = p_s/p_b \; [\frac{\delta\lambda}{\beta L} + \frac{p_a}{p_s}\frac{T_s}{T_a}] \; .$$

The pressure in the undisturbed region is the ambient; that in the post-shock region is determined from knowledge of the shock velocity; pressures are assumed to be applied down through the thermal layer for these uniform regions. For the multifringe interferogram, the fringe shifts from undisturbed fringe in both regions were calculated from an average slope determined for the undisturbed fringe. Ambient temperature before disturbance is assumed to be 300°K, although some temperature change of the air might be anticipated in the test section from the presence of the heated plate. Ambient temperature in the post-shock region is again from shock tables. Thus using such data in the temperature-fringe shift relation allows determination of the temperature profiles in pre-and post-shock regions of the thermal layer.

The region at the base of the shock and adjacent to the thermal layer requires separate consideration. Using the interferogram of

Figure 6 (with the infinite-fringe setting) for discussion, we noted that the fringes represent lines of constant density. Thus in this situation, an inverse analogy is suggested to the Mach waves or characteristics in steady two-dimensional flow over a gradual turn which intersect and coalesce into the main shock wave. Here, in the flow over the thermal layer - with temperature/sound speed gradient - we see disturbances from the main shock reaching down into the layer. The deep-lying subsonic portions of the layer must affect the disturbances such that acoustic waves propagate upstream in these portions, as evidenced by the small "breaks" in the fringes. Above these portions the propagation velocities must be supersonic, and the observed "fan" of weak shock waves propagate. Through velocity continuity considerations across any layer, one expects the leading or "precursor" nature of the shock pattern. Moreover, a succeeding weak wave moves at slower relative velocity (or has less an angle) since the wave leading has heated up, compressed, and set into motion the region ahead of the succeeding wave; hence it sees a smaller driving pressure ratio. In sum, the interferogram portrays in rather graphic form the complex shock-thermal layer interaction.

In view of this picture of a "transition" zone, we may make use of the weak shock relations to assign temperatures in this region. An implicit but not unreasonable assumption is that the region behind each weak shock is uniform. In the deep lying layers beneath the foot of the shock the pressure applied in the layers must vary somehow along the plate direction. Hence, adjustment of the temperature in these regions, from the uniform pre- and post-shock conditions, is unresolved in this work. The density "jump" at a fixed height in the deep-lying layers could be gotten from the fringe shift, as usual; but this has not been done. For the region spanned by the fan of weak shocks, the weak shock relations are

$$\frac{\Delta\rho}{\rho_a} = \frac{1}{\gamma} \frac{\Delta p}{p_a}$$

$$\frac{\Delta T}{T_a} = \frac{\gamma-1}{\gamma} \frac{\Delta p}{p_a} = (\gamma-1) \frac{\Delta\rho}{\rho_a}$$

which coupled with the fringe shift relation

$$\frac{\Delta\rho}{\rho_a} = \frac{\rho_s}{\rho_a} \frac{\lambda}{\beta L} \delta$$

give the working equations

$$T_b = [(\gamma-1)\frac{\rho_s}{\rho_a} \frac{\lambda}{\beta L}\delta + 1] T_a$$

14

and

$$\rho_b = \rho_s \frac{\lambda}{\beta L} \delta + \rho_a \quad .$$

The first calculation begins from the known undisturbed conditions. Succeeding flow values are obtained by iteration. The multifringe interferograms are treated in a similar manner. The results of such manipulations and of the experiments follow.

III. RESULTS AND DISCUSSION

Shown in Figure 7 are examples of completely reduced data runs. Accompanying each is the interferogram for the run. The shock velocity and Mach number are noted in the figures. The fringes sketched are scaled 4:1 of actual physical dimensions, as determined from the photographs and the known heated plate thickness, better to exhibit the temperature data. Temperature profiles in pre- and post-shock regions are illustrated. The temperature dependence for both regions appears generally to be an exponential decrease with increasing height above the plate, for about the first 0.75 cm, as the plots of Figure 8 show, and thereafter a decrease at a much slower rate until the ambient temperature is reached. Of note is the relatively good agreement of heated plate surface temperature T_p to either side of the shock. The infinite fringe interferograms exhibited greater disparity in the T_p, but values were well within 3% of each other. For the multifringe interferogram of Figure 7B, one may draw in local temperature contours in the transition zone, and most tend to straight lines, corroborating features of the infinite fringe interferograms. In the transition zone, in a majority of the runs the final temperature reached disagrees with the post-shock region temperature predicted from shock tables based on the measured shock velocity. Some of the discrepancy may be attributed to the cumulative error in stepping through the region. Other possible sources for error are discussed below.

Accuracy of the numbers generated is limited by several factors. Our knowledge of the initial, undisturbed, ambient conditions, particularly with heated plate in position, is a question. Beyond this, the shock speed is accurate to ± 1% as mentioned earlier; and comparator readings for fringe coordinates appear to be accurate and reproducible. The readings appeared to represent the fringe shapes faithfully, so that extrapolation of undisturbed (straight) fringes for determination of fringe shift should suffer no more than is usual. Of greater impact here is actually some curvature of fringes in the supposedly uniform regions, a feature noted in previous work in this facility[11] but not completely explained away. Areas with

---

11. *J. H. Spurk and J. M. Bartos, "Interferometric Measurement of the Nonequilibrium Flow Over a Cone." Phys. Fluids 9, 1278-85 (1966).*

noticeable fringe curvature were generally avoided, particularly at the field extremes.

Significant for the infinite fringe interferograms was that the interferometer setting, as it turned out after the run on several occasions, had drifted very slightly, with the result that several fringes, or some peculiar, large fringe pattern had set in, rather than the more or less evenly illuminated field desired (see Figure 6 and Figure 7C, post-shock region). Thus, the "zero" reference fringe from which the ensuing visible fringes have shifted is a somewhat questionable quantity. In order to reduce the data from such runs, a bit of interpretation was used to guess the reference fringe, based on the expected fringe shift through the shock, the height of the thermal layer above the heated plate, plus a count of fringes through the transition zone. Notwithstanding these uncertainties, one notes disturbances behind the shock in all the interferograms. One disturbance was traced to a shock reflection from a protruding gasket, subsequently re-positioned, upstream at the test section joint. A persisting disturbance was the shock reflection off the thickened "leading edge" of the plate caused by the thermal layer air currents around the edge. This effect is illustrated in the Figure 9. (Observation of the shocked flow over the cold plate itself showed no (blunt) leading edge effect at the test station, centered 25cm downstream of the leading edge.) Clearly, for very accurate work attention to the above mentioned uncertainties plus others would be required either to minimize or to estimate their effect on the experiment. The present work has, however, been exploratory and demonstrates some of the possibilities and the pitfalls associated with the shock/thermal layer interaction experiment and the interferometric technique for the desired temperature measurement. In the main, because of its familiarity and relative simplicity in data reduction procedures, the technique seems well suited for these studies.

Finally, some observations of the connection of the present experiments and results with field results should be made. The results and features protrayed in this work bear just some resemblance to precursor behavior in the field as depicted in Figure 1. Also, we have not attempted a comparison with the relation between precursor angle and temperature ratio, because of our non-uniform thermal layer. However, some tenuous correspondences might be drawn: The pressure levels in this work are appropriate to nuclear blasts at GR $\sim$ 600 m and beyond, where precursor behavior seems less pronounced. In Figure 10 are examples of pressure traces, from a shot with precursor formation, for such distances,[1] which are described as typical "clean-up" waveforms as the shock moves farther and farther from the source.

The ground level records 0B and 2B show a rather gradual rise to a plateau, followed by some indication of a cusp (more pronounced in 2B) (and subsequent drop-off associated with the spherical blast). The gradual pressure rise might correspond to the undetermined

pressure development implied by the interferograms in passing from the pre-shock region to the post-shock region along the heated plate surface. The cusp might then be identified with the small break mentioned earlier in the fringes deep in the heated layer.

The above ground stations 2B10 and 2B50 show the pressure rise and increase in pressure to a second sharp rise before the pressure decrease of the spherical blast. The transition zone behavior depicted in the interferograms would correspond thusly: the initial and rising pressures are those associated with the first and subsequent waves of the transition region. The sharper second pressure rise at greater height would signify the lessened influence at greater height of the thermal layer i.e.,the lessened extent of the wave "fan" from the main shock and the more normal-shock behavior of the disturbance.

Additionally, shock contours plotted from direct shock photography of nuclear bursts show some interesting features. Figure 11 reproduces a few pertinent ones from a Figure in Reference 1, which shows, for a shot, shock contours and their heights at various ground ranges; times after burst are also indicated. In particular, we note the multiple shocks fanning down from single, main shocks, bearing rather clear similarity to the shocks of the transition zone in the present experiments. In the field tests a number of density gradients were seen behind the leading precursor wavefront at any instant. Many of these were thought to be local disturbances. The results of our experiments suggest another likelihood also: that the density gradients, or equivalently, the thin regions constituting the transition zone are intimately connected with the interactions between the main shock and the thermal layer and not solely with particular, local disturbances. We stress that these remarks are somewhat speculative, and no additional evidence is presently in hand to support them.

IV. CONCLUSIONS

This report, based on observations using a Mach Zehnder interferometer, examines some features of the interaction of a plane shock generated by a shock tube with a thermal layer created over a heated plate. The technique is similar to that of Griffith who worked at much lower temperatures. Temperature profiles through the thermal layer are determined in the pre- and post-shock regions. The interferograms show a feature of the interaction - a "transition zone" which is interpreted as a decomposition of the main shock into a fan of weak shock or Mach waves reaching down into the thermal layer. Some of the waves "lead" the main shock and would be associated with the normally observed "precursor" shock. Some assumptions are made to assign temperatures in this transition zone. Tentative connections of the experimental results with field results are discussed.

17

ACKNOWLEDGMENTS
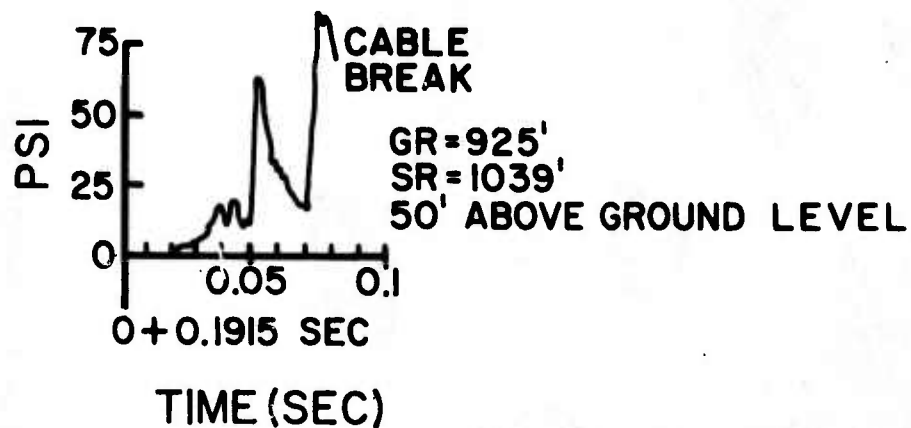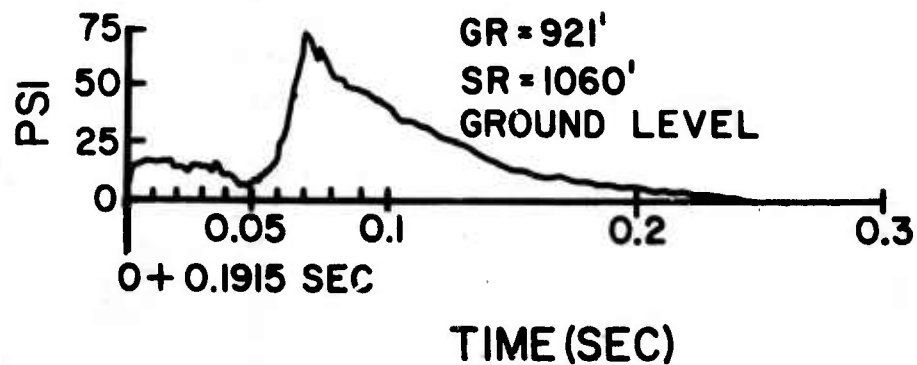
Figure 1. Representative Pressure-Time Records Exhibiting
Precursor Shock from Nuclear Burst

19
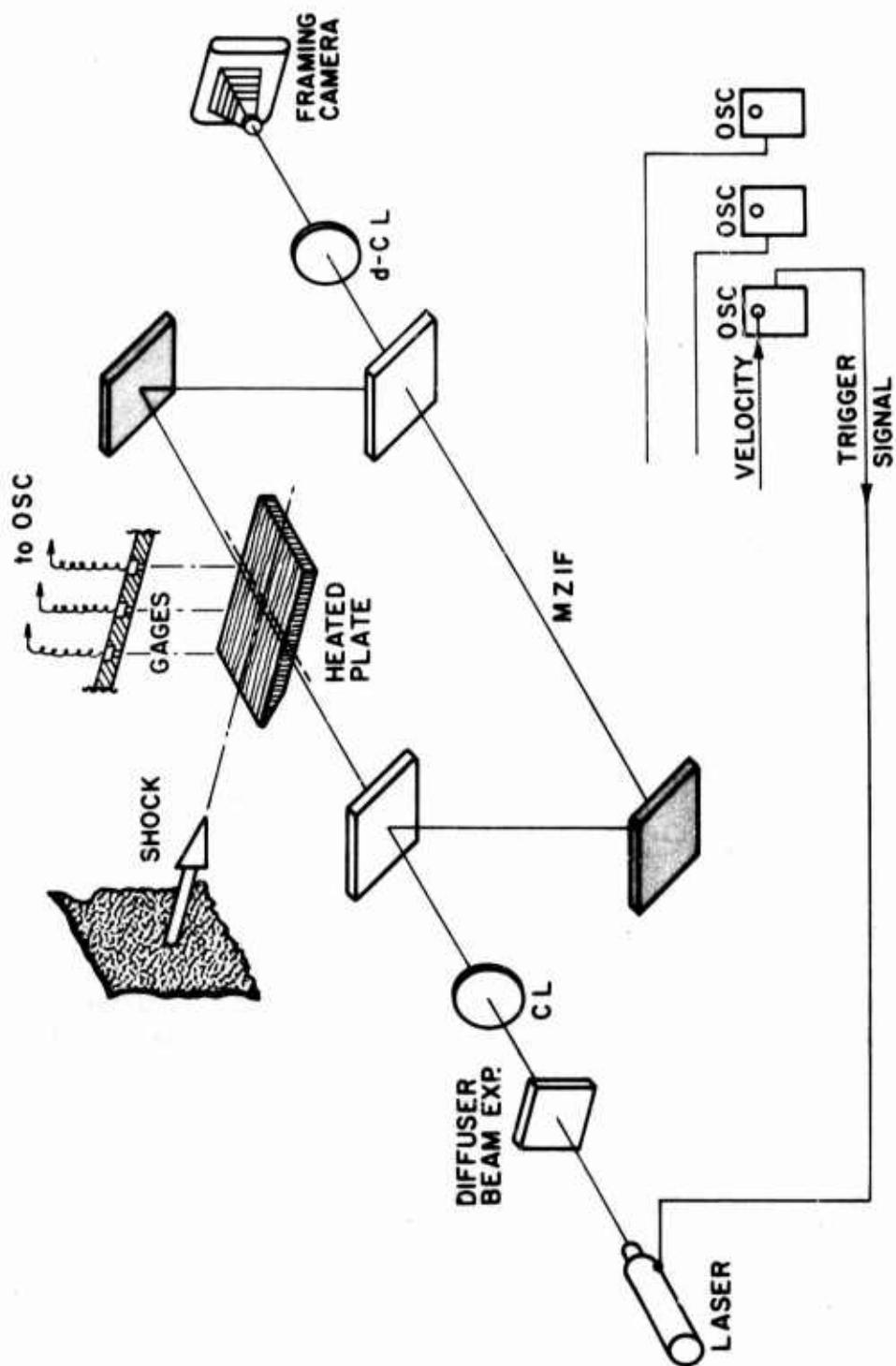
Figure 2. Overall Sketch of Experimental Apparatus
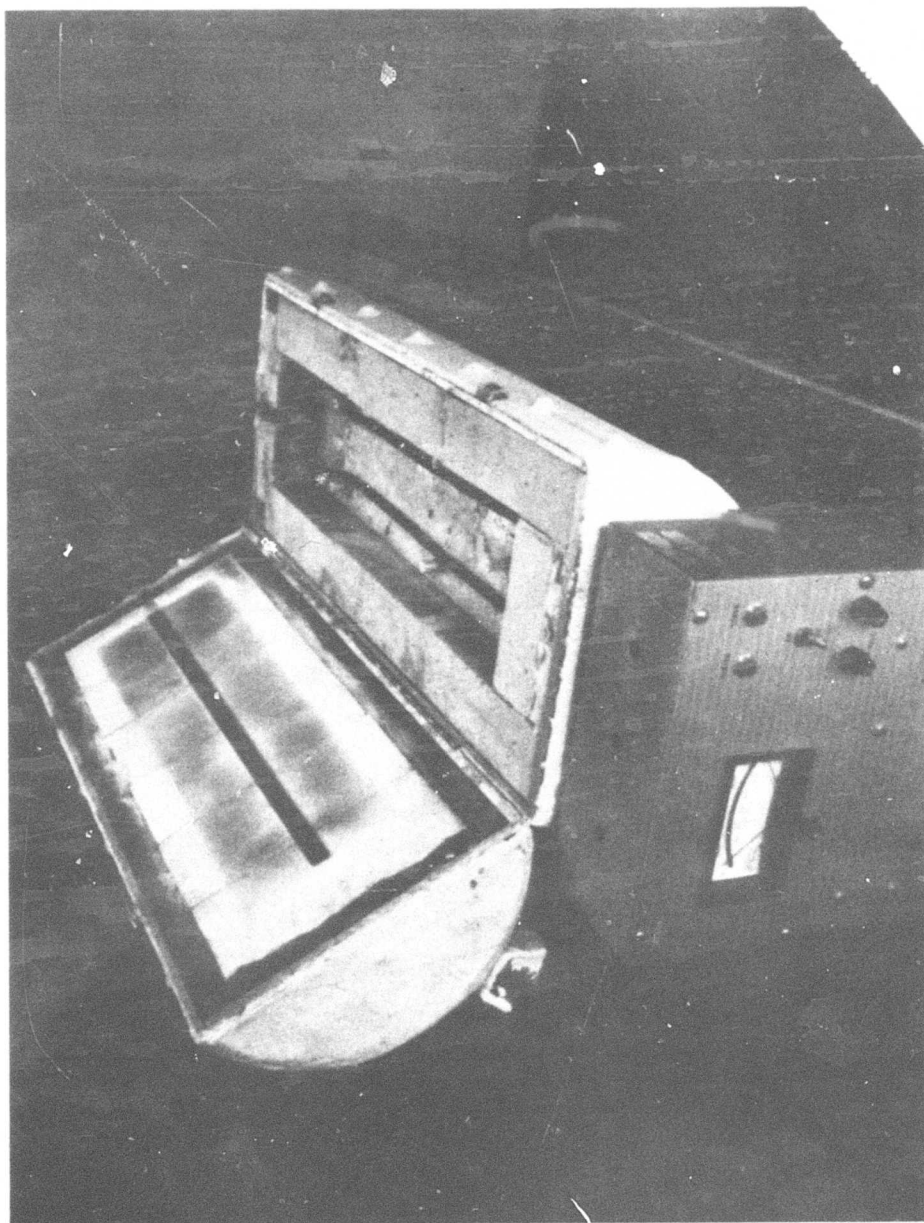
Figure 3. Oven for Heating Steel Test Plate
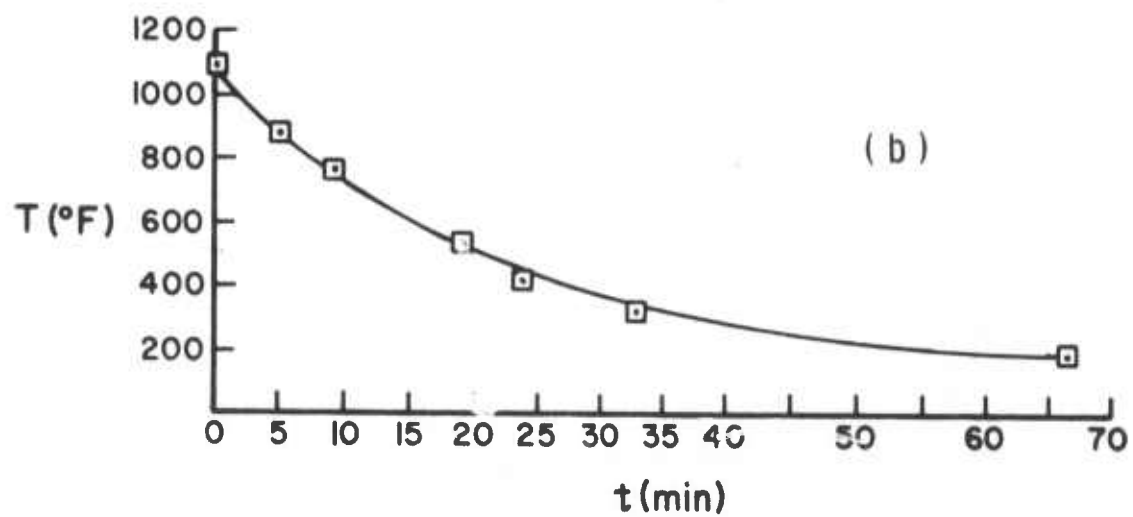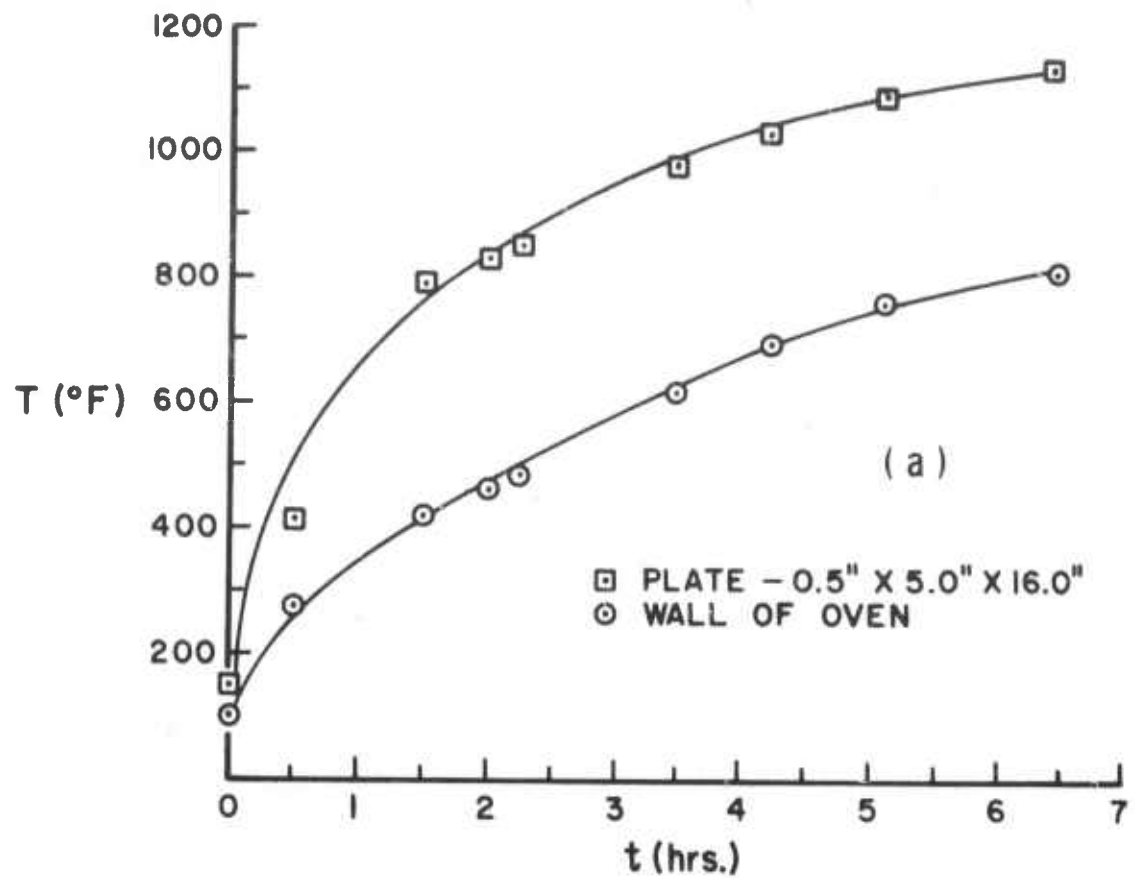
Figure 4.   Heating/Cooling Curves for Oven and Test Plate

GAGE 1

GAGE 2

100 μsec

GAGE 2

100 μsec

LASER
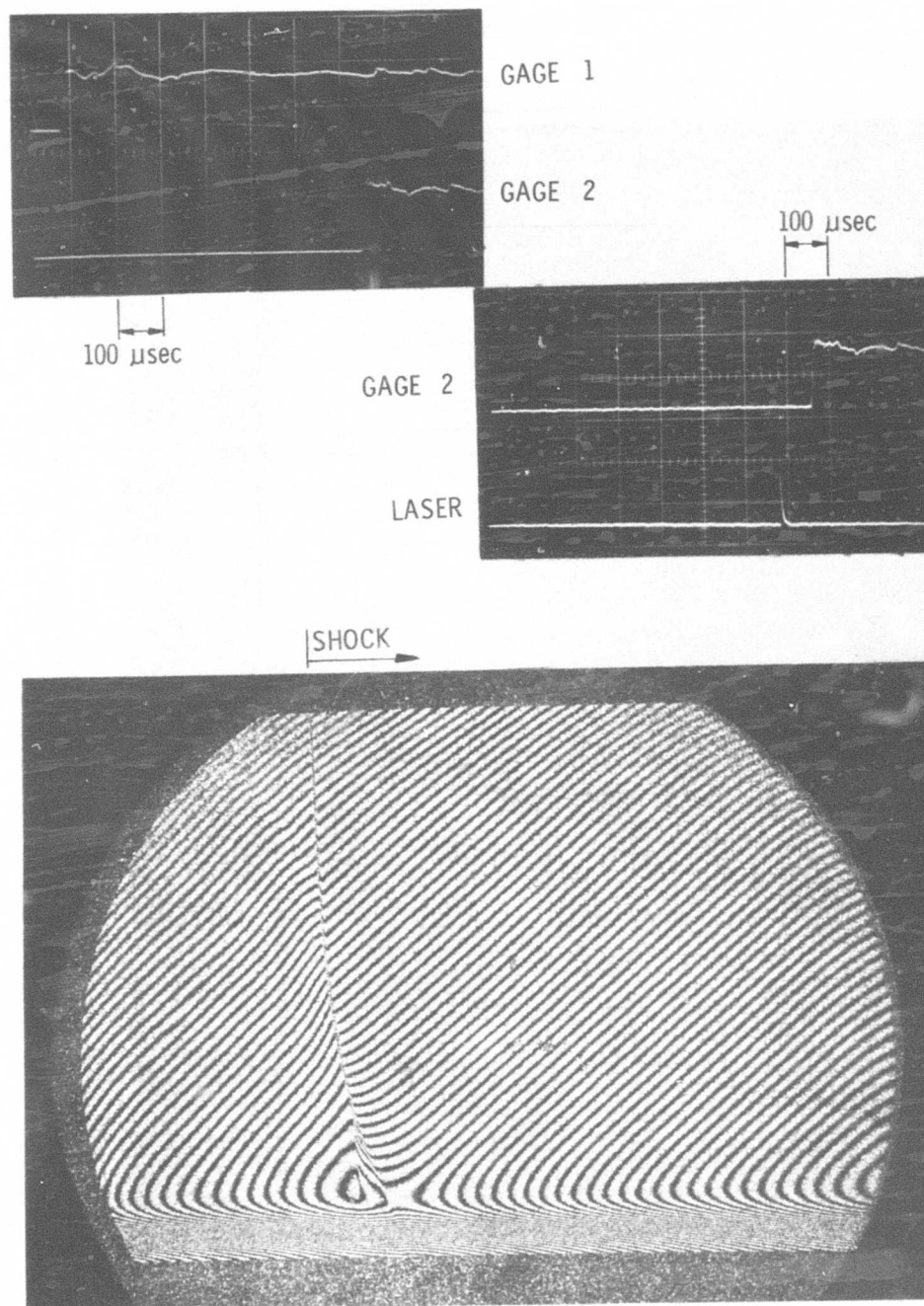
|SHOCK →

Figure 5. Typical Records for a Run

23
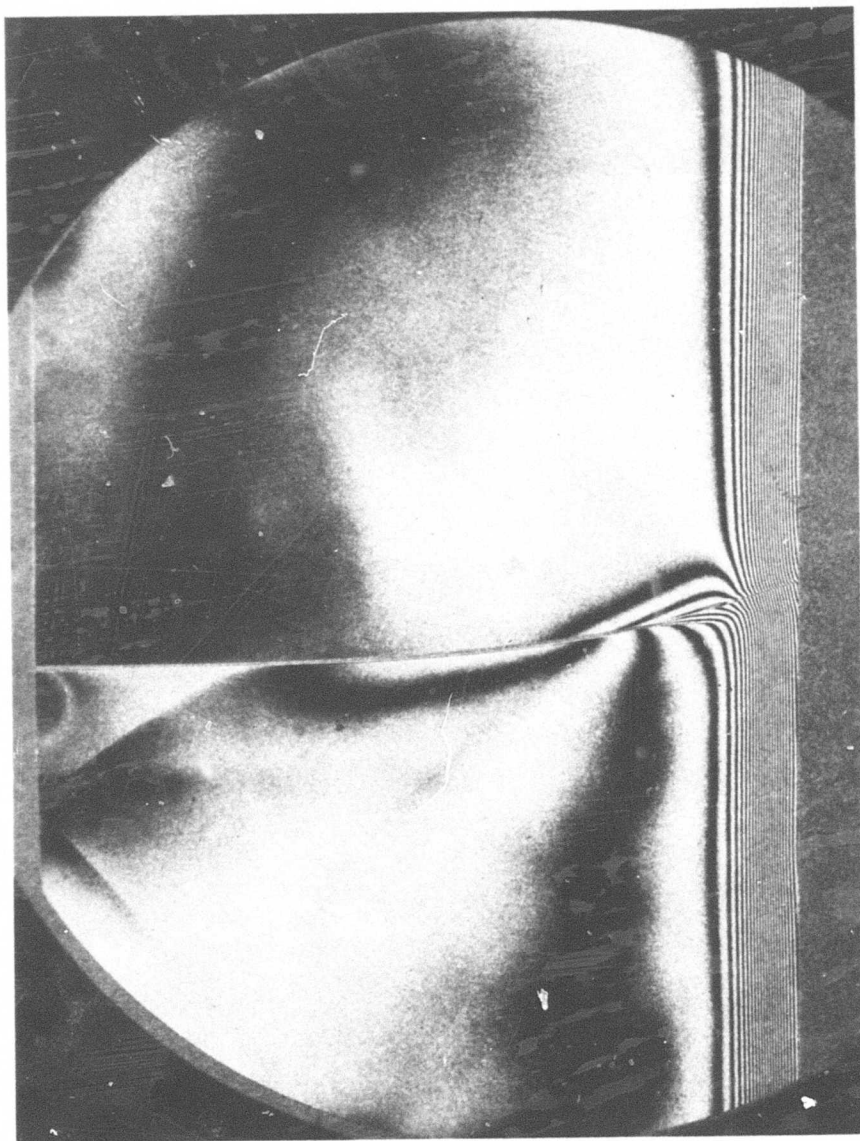
Figure 6.   Sample Infinite – Fringe Interferogram

Post-Shock
Temp.
Profile
y(in) T(°K)

0.80 —
0.70 —
0.60 —
0.50 —
0.40 — 320
        327
0.30 — 338
        350
        370
0.20 — 402
0.10 — 428
0.05 — 454
0 — 476

325

321
318
306 303

Temp. in
"Transition
Region"

V_S

$V_S = 384 \, m/s$
$M_S = 1.103$
$T_2/T_1 = 1.067$
x,y scales: 1.0" figure = 0.25"

Pre-Shock
Temp.
Profile
T(°K)   y(in.)

300 — 0.6
301 — 0.5
304 —
307 — 0.4
312 —
318 — 0.3
329 —
346 — 0.2
367 —
392 —
423 — 0.1
458 — 0.05
488 — 0

Figure 7A-1. Completely Reduced Data Runs and Interferograms Showing Temperatures in Various Regions of the Shock-Thermal Layer

Figure 7A-2. Completely Reduced Data Runs and Interferograms Showing Temperatures in Various Regions of the Shock-Thermal Layer

$V_S = 385\,m/s$

$M_S = 1.106$

$T_2/T_1 = 1.068$

x,y scales: $1''$Fig. $= 0.25''$

$V_S \longrightarrow$

Pre-Shock Temp Profile
$T(°K)\ y(in.)$

300	1.0
300	0.75
302	0.50
304	0.40
314	0.30
330	
353	0.20
382	
420	0.10
468	
527	
600	
678	0

Post-Shock Temp Profile
$y(in.)\ T(°K)$

1.0	320
0.75	319
	320
	320
	321
	323
0.50	324
	328
0.40	338
	354
0.30	375
	407
0.20	450
	508
0.10	560
	620
0	675

320 318 313 310 314
303 302 301 300
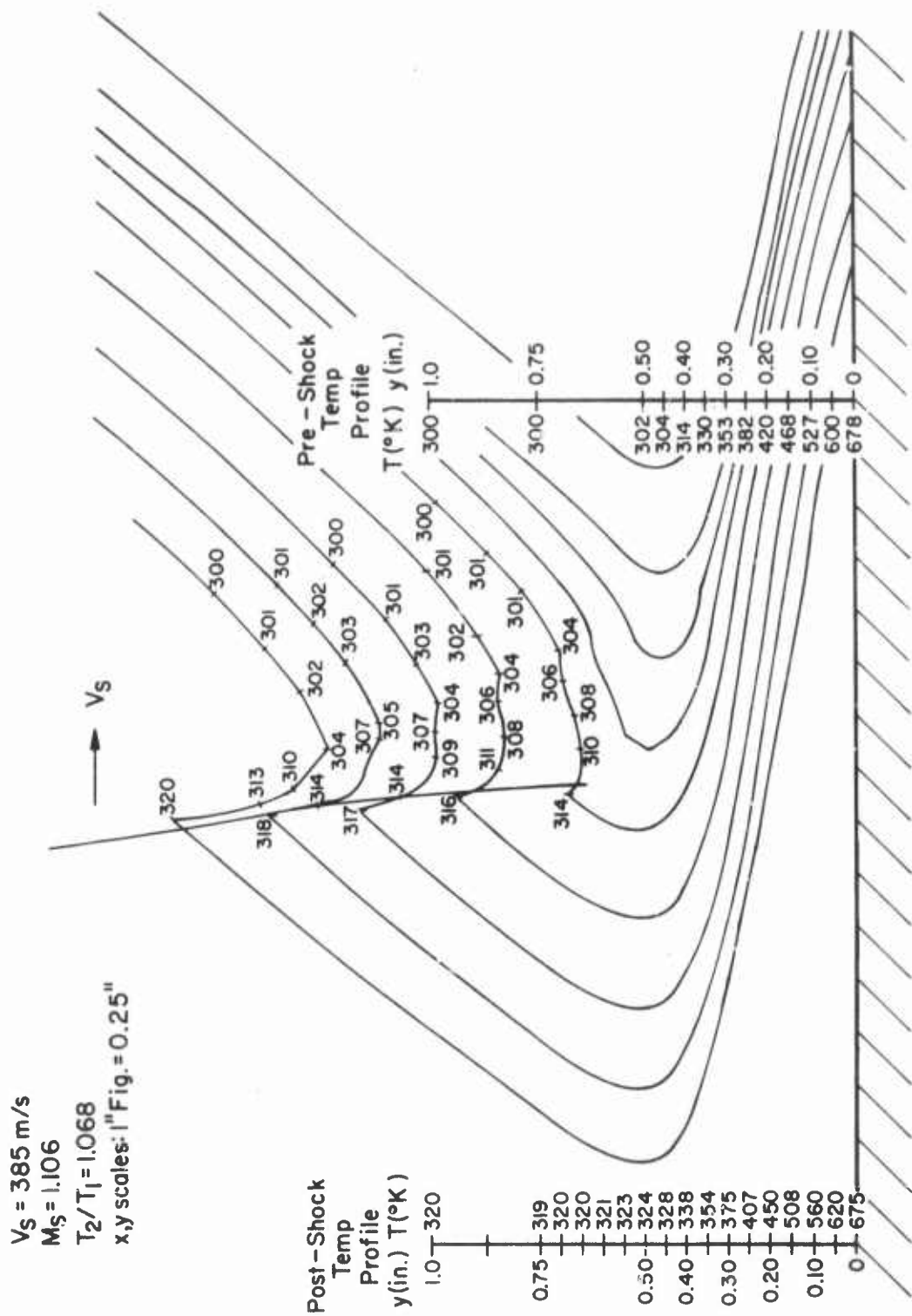
Figure 7B-1. Completely Reduced Data Runs and Interferograms Showing Temperatures in Various Regions of the Shock-Thermal Layer

27
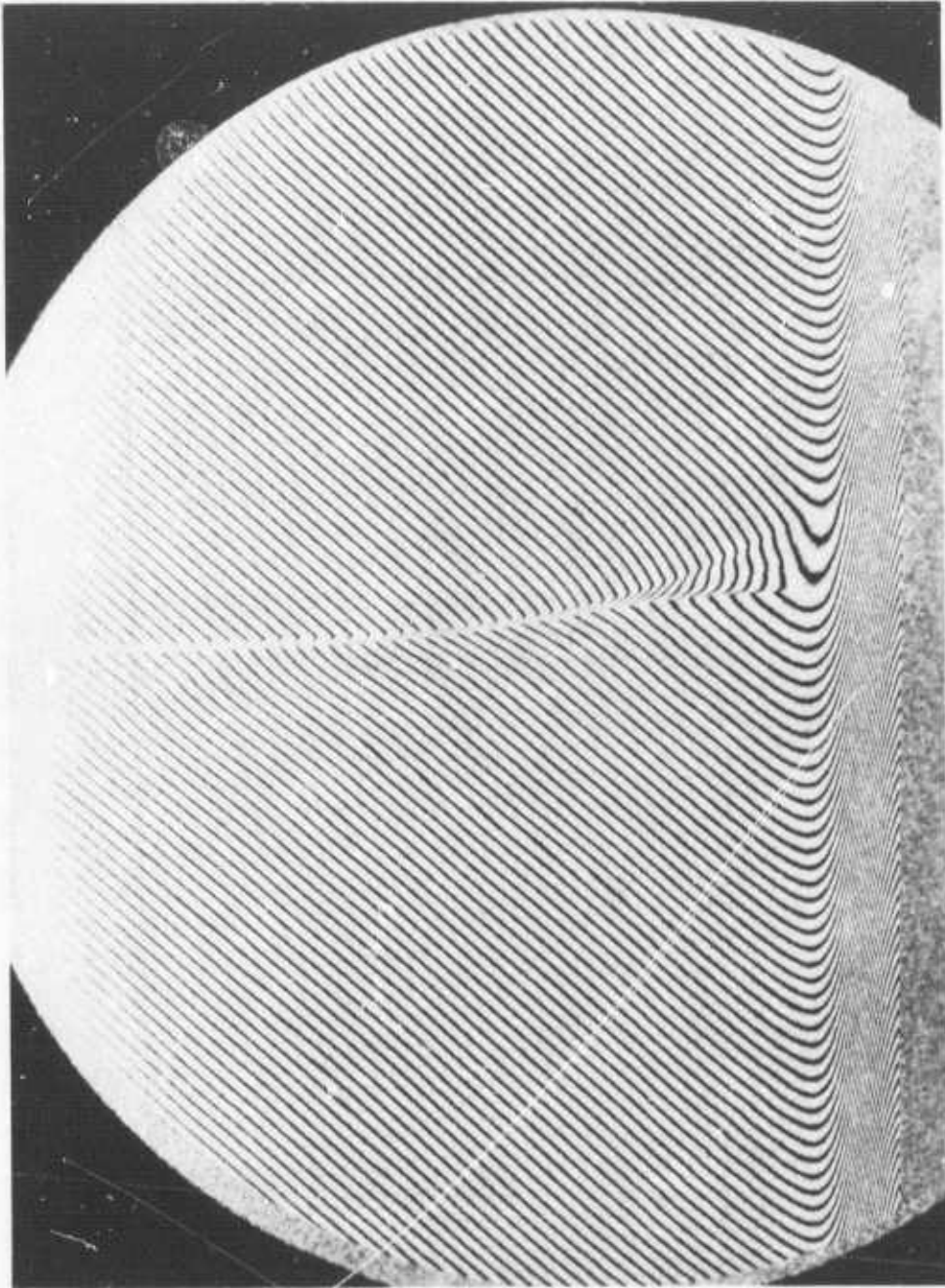
Figure 7B-2. Completely Reduced Data Runs and Interferograms Showing Temperatures in Various Regions of the Shock-Thermal Layer

$V_S = 400 \, \text{m/s}$

$M_S = 1.149$

$T_2 / T_1 = 1.096$

x,y scales: 1" Fig. = 0.25"

Pre-Shock Temp Profile
T(°K) y(in.)

T(°K)	y(in.)
	1.0
	0.90
	0.80
	0.70
310	0.60
313	0.50
318	
326	0.40
340	
360	0.30
395	
438	0.20
502	
572	0.10
668	
763	
905	0

Post-Shock Temp. Profile
y(in.) T(°K)

y(in.)	T(°K)
1.0	
0.90	
0.80	335
0.70	336
	338
0.60	340
	344
0.50	353
	370
0.40	402
	445
0.30	498
	562
0.20	640
	728
0.10	793
	860
0	885

Temp. in Transition Region

300

303

309

315

321

326

332

337
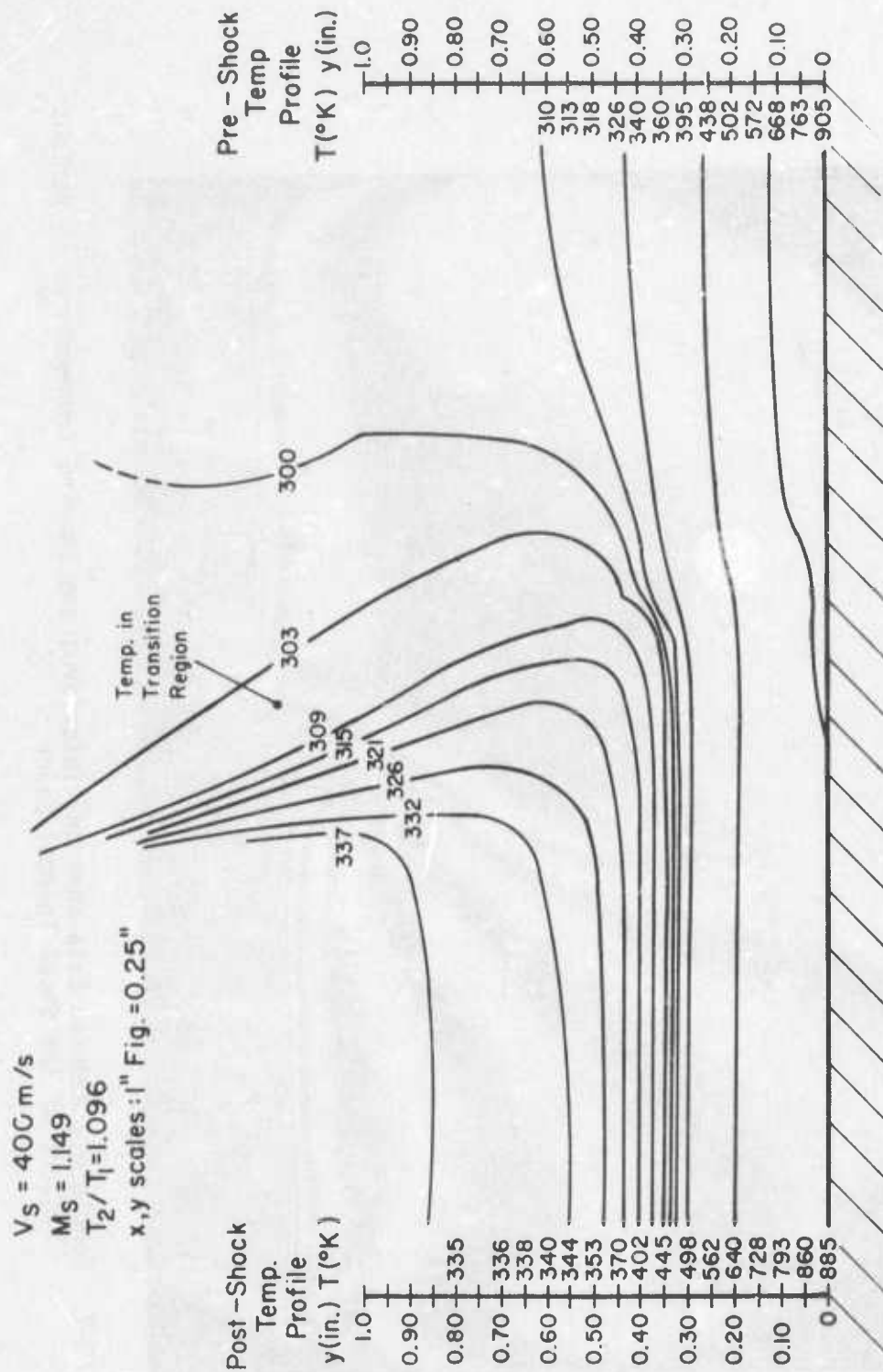
Figure 7C-1. Completely Reduced Data Runs and Interferograms Showing Temperatures in Various Regions of the Shock-Thermal Layer
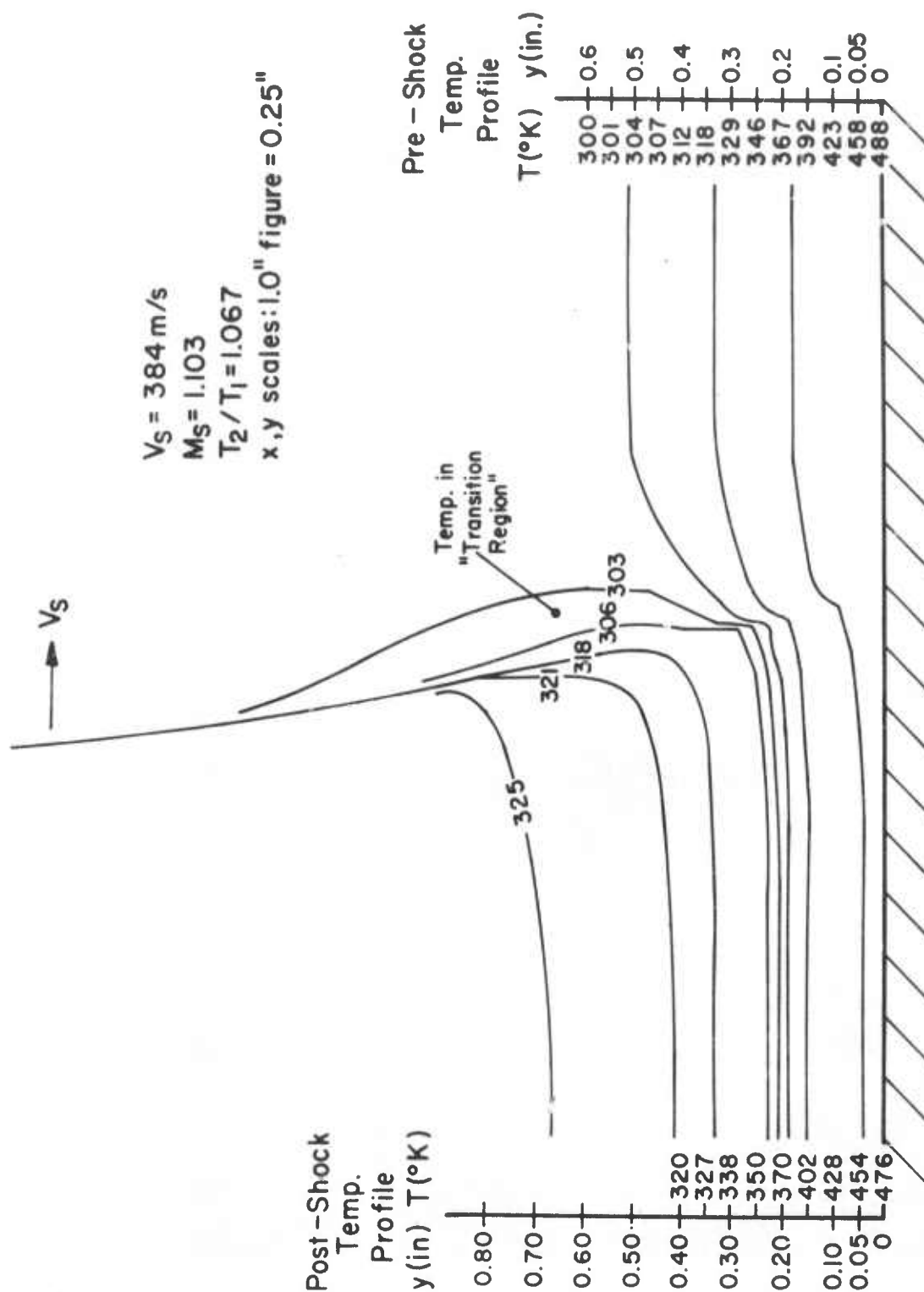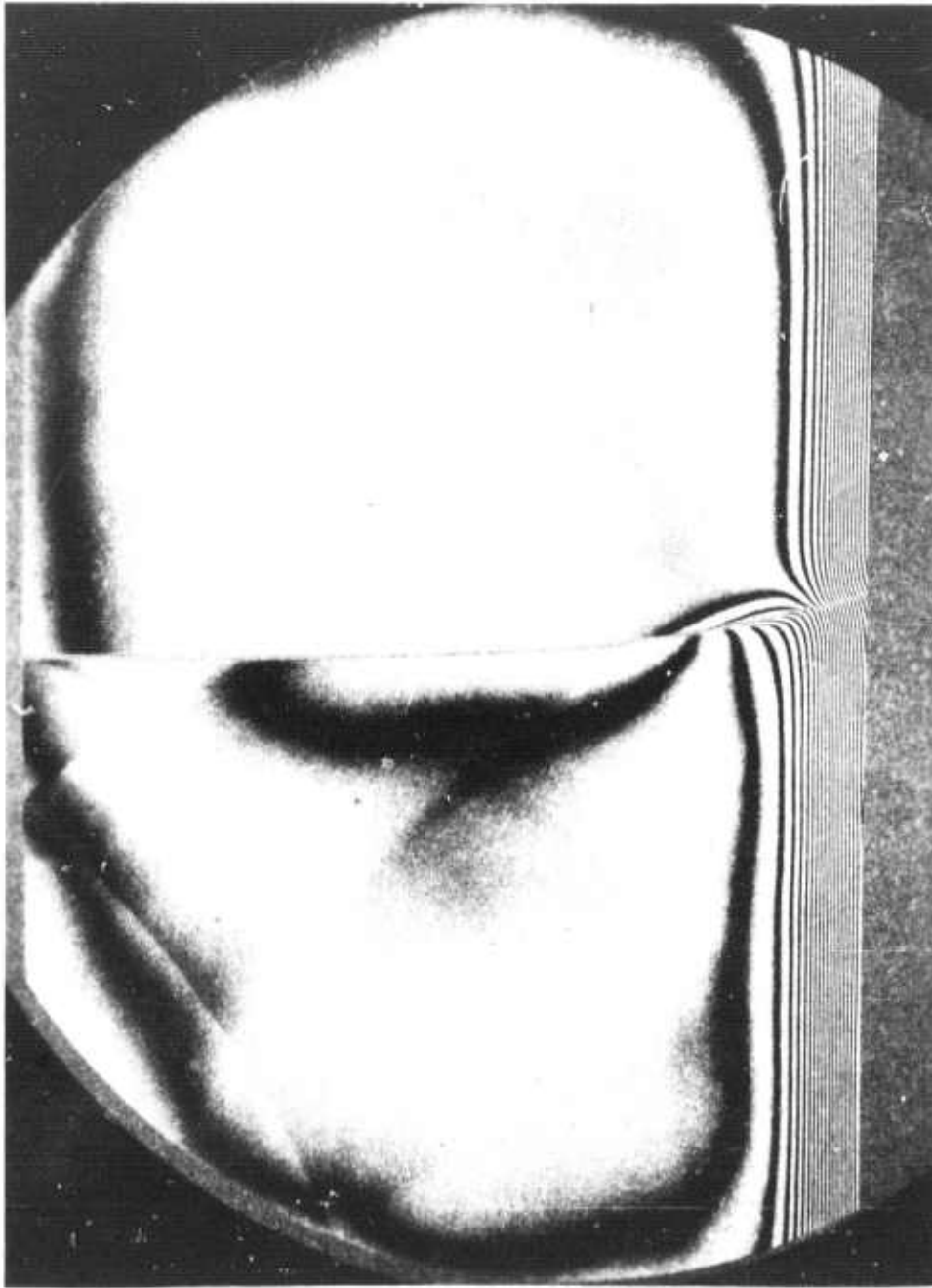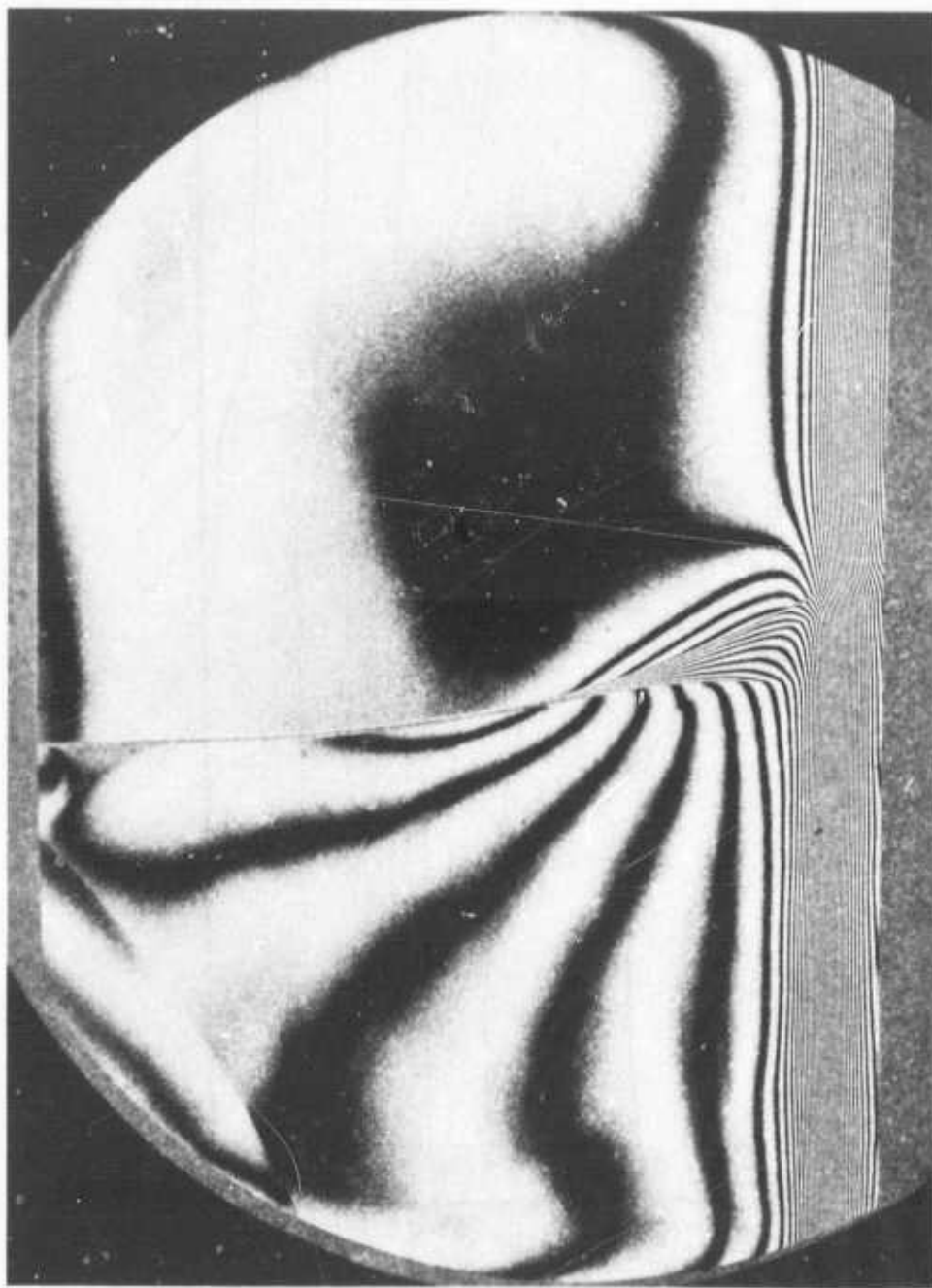
Figure 7C-2. Completely Reduced Data Runs and Interferograms Showing Temperatures in Various Regions of the Shock-Thermal Layer
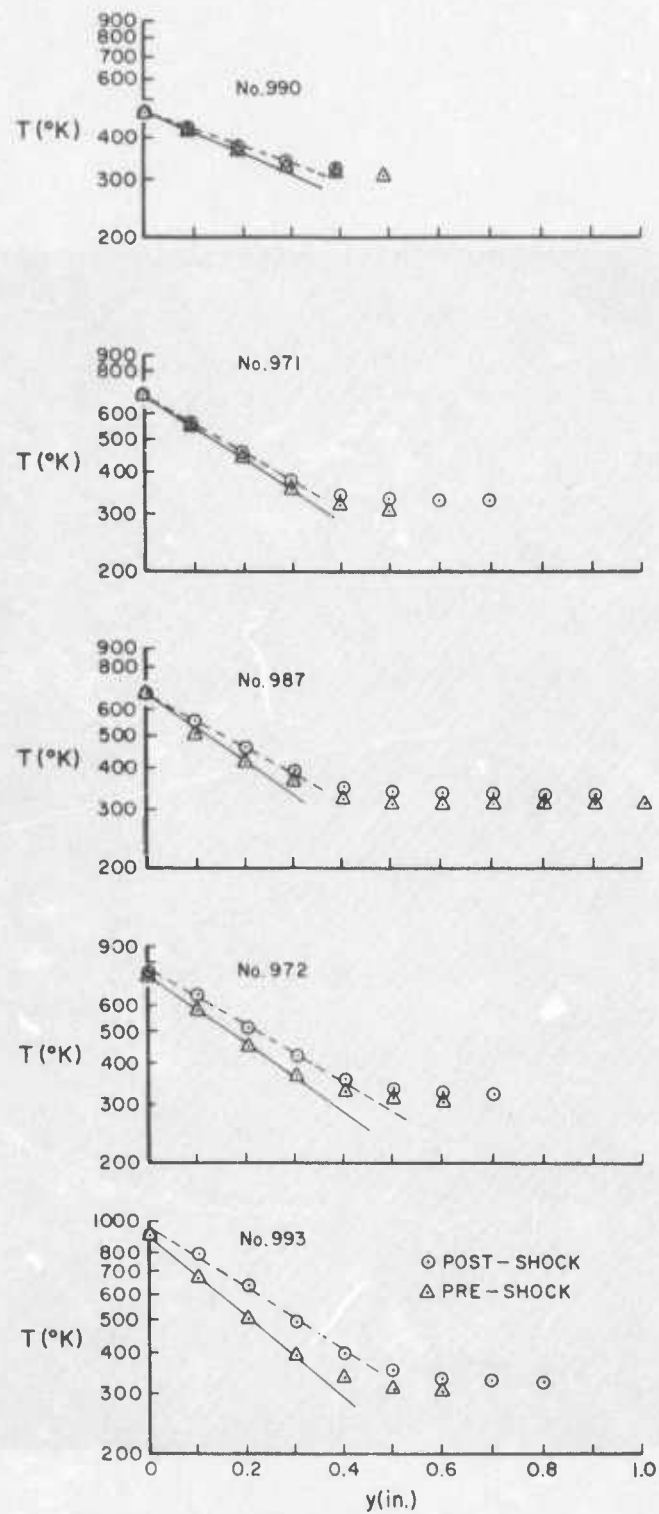
Figure 8. Temperature Dependence of Heated Layer in Pre- and Post-Shock Region
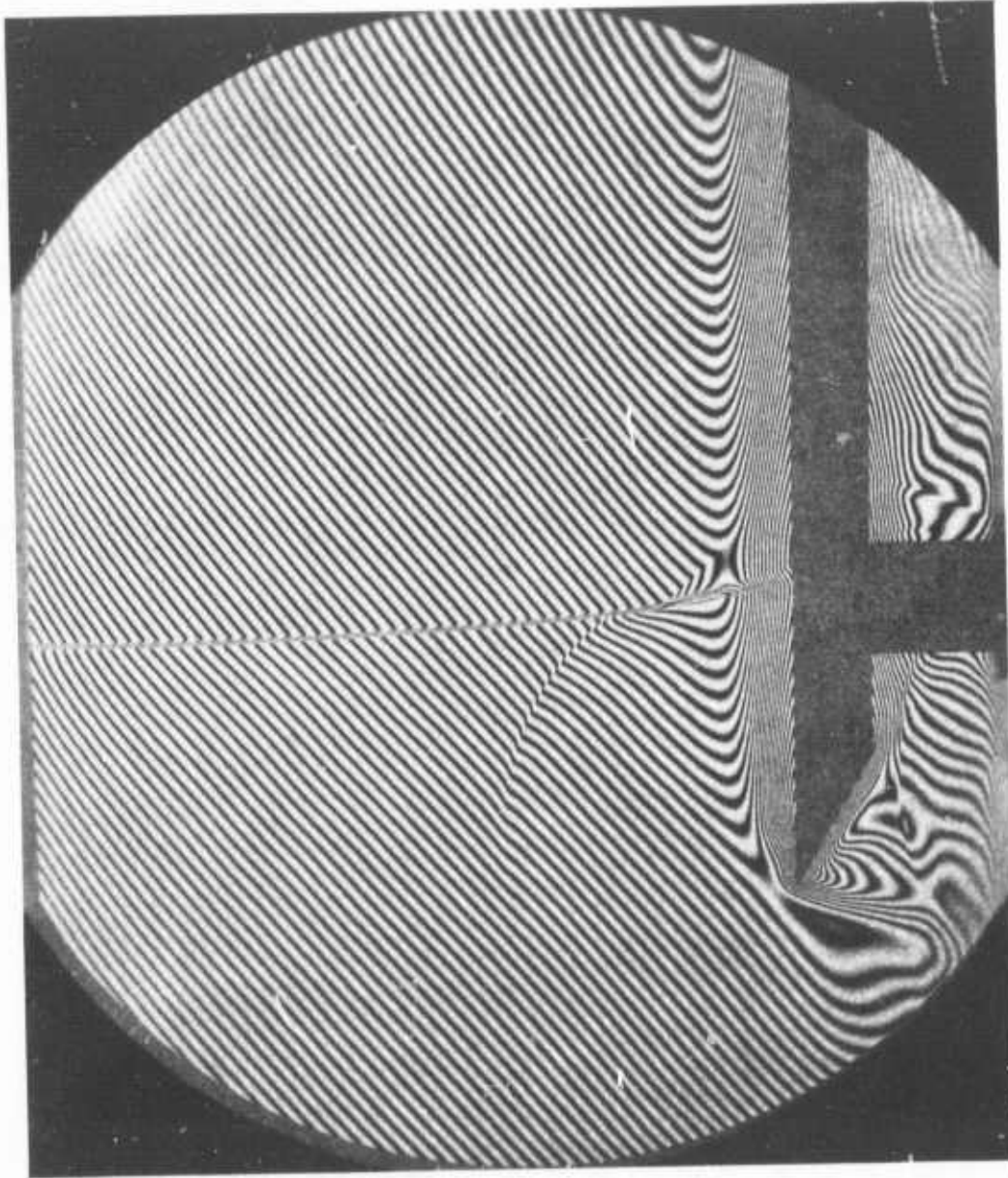
Figure 9. Shock Reflection off "Leading Edge" of Plate

OB
GR = 1918'
SR = 1988'

O + 0.596 SEC.

OB 50
GR = 1919'
SR = 1977'

O + 0.596 SEC.

2B
GR = 2417'
SR = 2473'

O + 0.974 SEC.

2B 10
GR = 2418'
SR = 2472'

O + 0.974 SEC

2B 50
GR = 2418'
SR = 2464'

O + 0.974 SEC.

TIME(SEC)
GR = GROUND RANGE FROM GZ
SR = SLANT RANGE FROM BURST
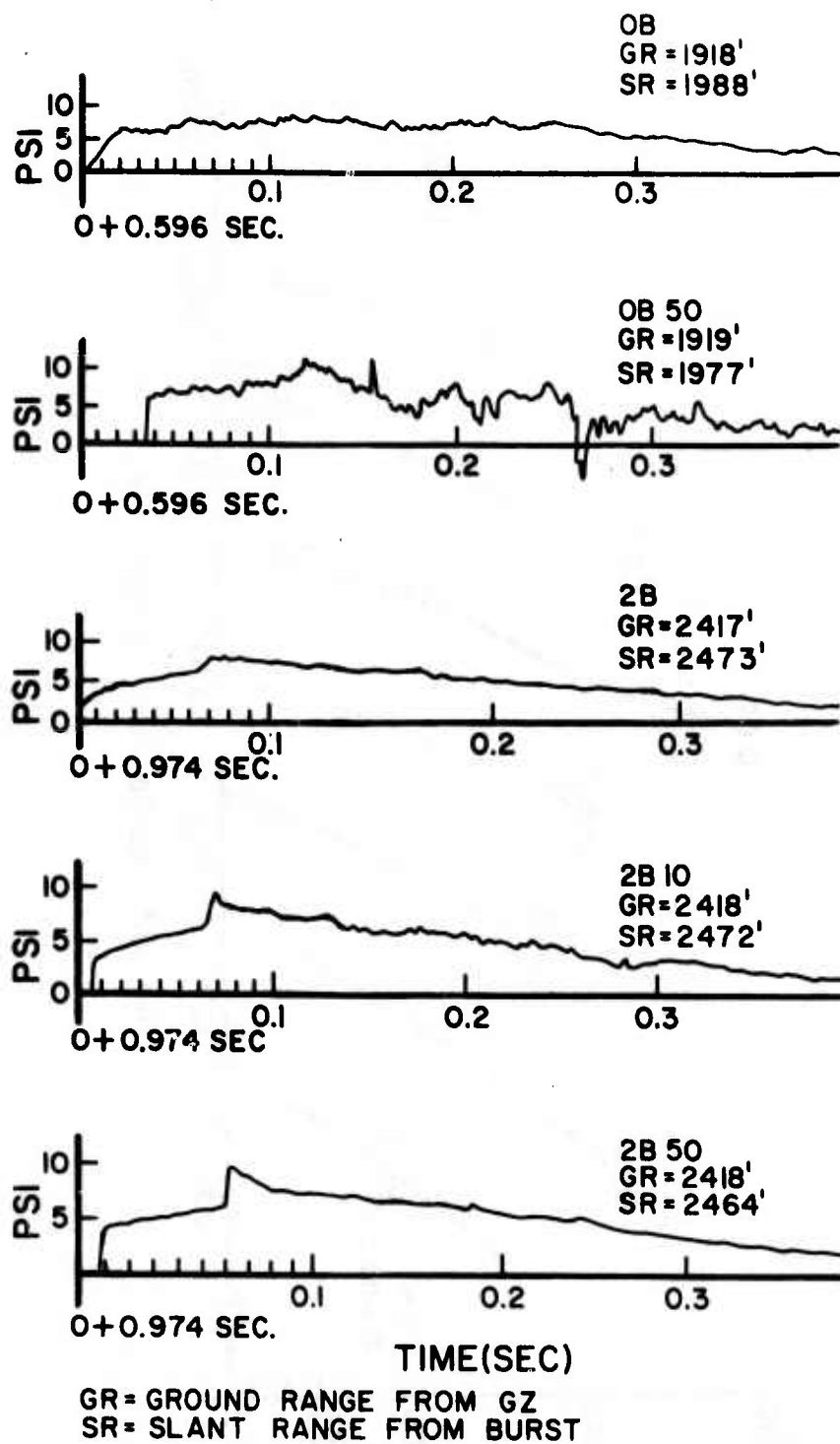
Figure 10. Other Precursor Waveforms at GR $\gtrsim$ 600 m.

33
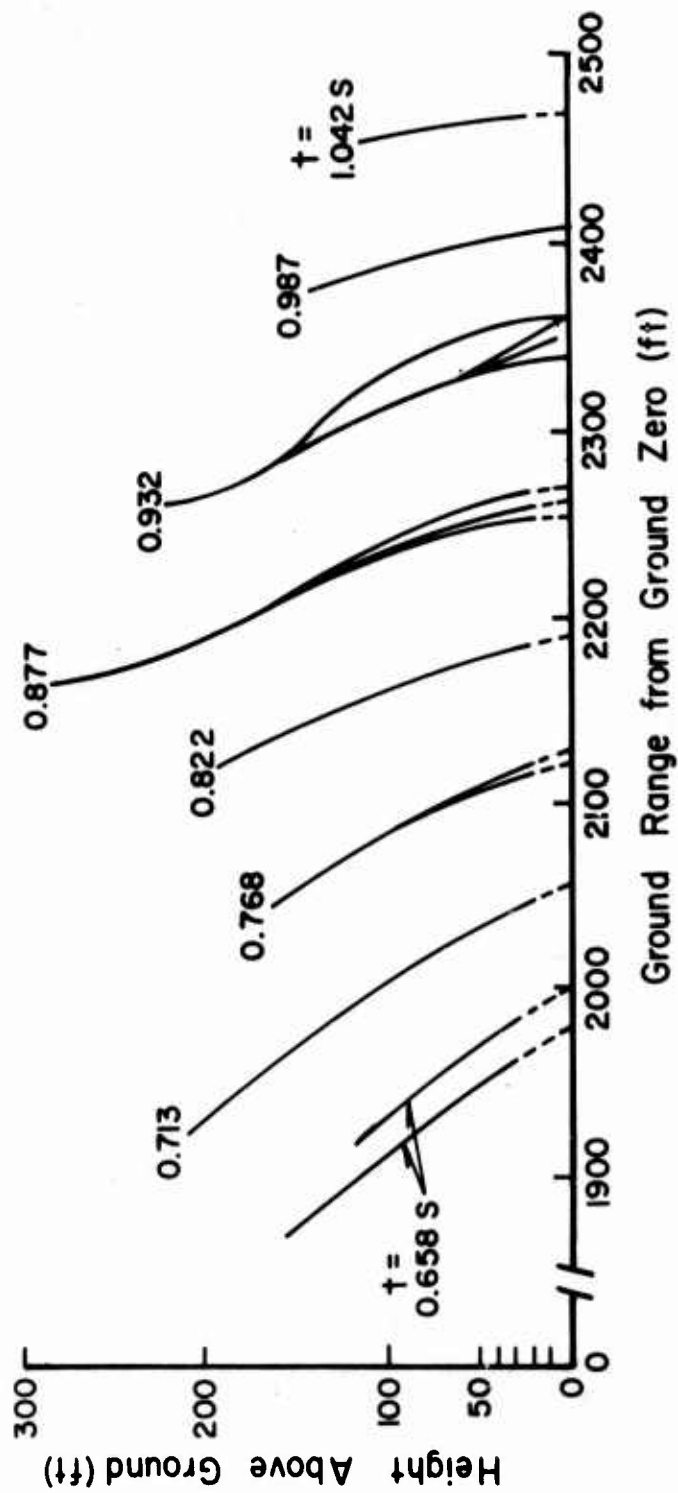
Figure 11. Shock Contours from a Nuclear Burst

34

REFERENCES

1. K. Kaplan, P. J. Norris, P. A. Ellis, and D. C. Sachs, "Nuclear Blast Phenomena - Vol. II." DASA 1200 (1971). CONFIDENTIAL.

2. T. R. Broida, A. Broido, and A. B. Willoughby, "Air Temperature in the Vicinity of a Nuclear Detonation" Operation TUMBLER Project 8.2WT542.

3. E. C. Y. Inn, "Air Temperature Measurements Over Several Surfaces." Operation TEAPOT Project 8.4e WT-1149 (1957).

4. W. C. Griffith, "Interaction of a Shock Wave with a Thermal Boundary Layer." J. Aero. Sci. 23, 16-23 (1956).

5. R. Varwig and J. Zemel, "The Interaction of Shock Waves with a Thermal Layer." NAVORD Report 4021, AFSWR266 (1955).

6. R. G. Jahn, "The Refraction of Shock Waves at a Gaseous Interface - III. Irregular Refraction." Princeton University Tech. Report II-19 (1955).

7. L. Howarth, "The Propagation of Steady Disturbances in a Supersonic Stream Bounded on One Side by a Parallel Subsonic Stream." Proc. Cambr. Phil. Soc. 44, 380-90 (1948).

8. H. S. Tsien and M. Finston, "Interaction Between Parallel Streams of Subsonic and Supersonic Velocities." J. Aero. Sci. 16, 515-528 (1949).

9. F. H. Oertel, "Laser Interferometry of Unsteady Underexpanded Jets." BRLR 1694 (1974) AD 773664.

10. T. A. Wiggins, "Methods for Spreading Laser Beams." Appl. Optics 10, 963-5 (1971).

11. J. H. Spurk and J. M. Bartos, "Interferometric Measurement of the Nonequilibrium Flow Over a Cone." Phys. Fluids 9, 1278-85 (1966).

DISTRIBUTION LIST

No. of Copies	Organization
12	Commander Defense Documentation Center ATTN: DDC-TCA Cameron Station Alexandria, VA 22314
4	Director of Defense Research and Engineering ATTN: DD/TWP DD/S&SS DD/T&SS AD/SW Washington, DC 20301
6	Director Defense Nuclear Agency ATTN: STTL (Tech Lib, 2 cys) SPAS, Mr. J. Moulton DDST, Mr. P. H. Haas SPTD, Mr. J. Kelso SPAS, Mr. D. Kohler Washington, DC 20305
3	Director Defense Advanced Research Projects Agency ATTN: Tech Library NMRO PMO 1400 Wilson Boulevard Arlington, VA 22209
2	Commander Field Command, DNA ATTN: FCPR Mr. Noel Ganick Kirtland AFB, NM 87115
2	Department of Defense Explosives Safety Board ATTN: R. Perkins Dr. Tom Zaker Room GB-270, Forrestal Bldg Washington, DC 20314

No. of Copies	Organization
1	Commander US Army Materiel Development and Readiness Command ATTN: DRCDMA-ST 5001 Eisenhower Avenue Alexandria, VA 22333
1	Commander US Army Aviation Systems Command ATTN: DRSAV-E 12th and Spruce Streets St. Louis, MO 63160
1	Director US Army Air Mobility Research and Development Laboratory Ames Research Center Moffett Field, CA 94035
4	Commander US Army Electronics Command ATTN: DRSEL-RD DRSEL-IR, J. Roma DRSEL-TL, S. Kronenberg R. Freiberg Fort Monmouth, NJ 07703
4	Commander US Army Missile Command ATTN: DRSMI-S, Ch Scientist DRSMI-R DRSMI-RR, L. Lively DRSMI-RKP, W. Thomas Redstone Arsenal, AL 35809
2	Commander US Army Tank Automotive Development Command ATTN: DRDTA-RHT, LT P. Hasek DRDTA-RWL Warren, MI 48090

DISTRIBUTION LIST

No. of Copies	Organization	No. of Copies	Organization
2	Commander US Army Mobility Equipment Research & Development Command ATTN: Tech Docu Cen, Bldg 315 DRSME-RZT Fort Belvoir, VA 22060	3	Commander US Army Nuclear Agency ATTN: ATCN-W/CPT M. Bowling CDINS-E Technical Library Fort Bliss, TX 79916
1	Commander US Army Armament Command ATTN: SARRI-LR/Mr. B. Morris Rock Island, IL 61202	1	Director US Army TRADOC Systems Analysis Activity ATTN: ATAA-SA White Sands Missile Range NM 88002
2	Commander US Army Picatinny Arsenal ATTN: P. Angelotti SARPA - Mr. G. Demitrack Dover, NJ 07801	1	HQDA (DAMA-AR, NCB Div.) Washington, DC 20310
5	Commander US Army Harry Diamond Labs ATTN: DRXDO-TI DRXDO-TI/012 DRXDO-NP, F. N. Wimenitz DRXDO-NP, Jim Gaul DRXDO-NP, J. H. Gwaltney 2800 Powder Mill Road Adelphi, MD 20783	1	Director US Army Advanced BMD Technology Center ATTN: Technical Library Commonwealth Building 1320 Wilson Boulevard Arlington, VA 22209
1	Director US Army Materials and Mechanics Research Center ATTN: Technical Library Watertown, MA 02172	3	Director US Army Advanced BMD Technology Center ATTN: Mr. B. E. Kelley Mr. M. Capps Mr. Marcus Whitfield P.O. Box 1500 Huntsville, AL 35807
1	Commander US Army Foreign Science and Technology Center ATTN: Research & Data Branch 220 - 7th Street, NE Charlottesville, VA 22901	1	Commander US Army Ballistic Missile Defense Program Office ATTN: DACS-SAE-S, J. Shea Commonwealth Building 1300 Wilson Boulevard Arlington, VA 22209

DISTRIBUTION LIST

No. of Copies	Organization	No. of Copies	Organization

3   Commander
US Army Ballistic Missile
    Defense Systems Command
ATTN: SSC-DRS, J. G. Buxbaum
        SSC-DH, H. L. Solomonson
        SSC-HS, H. Porter
P.O. Box 1500
Huntsville, AL 35807

1   Commander
US Army Ballistic Missile
    Defense Systems Evaluation
    Agency
ATTN: Mr. R. E. Dekinder, Jr.
White Sands Missile Range
NM 88002

2   Commander
US Army Engineer Waterways
    Experiment Station
ATTN: Library
       Mr. W. Flateau
P.O. Box 631
Vicksburg, MS 39180

3   Chief of Naval Research
Department of the Navy
ATTN: T. Quinn, Code 464
       Technical Library
       J. L. Warner, Code 464
Washington, DC 20360

2   Commander
Naval Ship Engineering Center
ATTN: J. R. Sullivan, NSEC
       6105-G
       Technical Library
Hyattsville, MD 20782

3   Commander
US Naval Surface Weapons Center
ATTN: Code 1224, Navy Nuclear
       Programs Office
       Code 241, J. Petes
       Code 730, Tech Library
Silver Spring, MD 20910

1   Commander
Naval Weapons Evaluation Facility
ATTN: Document Control
Kirtland AFB, NM 87117

2   Commander
Naval Civil Engineering Lab
ATTN: Dr. W. A. Shaw, Code L31
       R. Seabold
Port Hueneme, CA 93041

3   Director
US Naval Research Laboratory
ATTN: M. Persechino
       G. Cooperstein
       Tech Library/Code 2027
Washington, DC 20390

1   Commander
Charleston Navy Shipyard
ATTN: H. Shuler
Charleston, SC 29451

1   HQ USAFSC (DLCAW)
Andrews AFB
Washington, DC 20331

1   AFOSR (OAR)
Bolling AFB, DC 20332

1   RADC (Documents Library) FMTLD
Griffiss AFB, NY 13440

1   AFGL
ATTN: F. Doherty
Hanscom AFB, MA 01731

4   AFWL (WLRE, Dr. A. Guenther;
    DYT, Charles Needham;
    DYT, MAJ G. Ganong;
    DYT, Burt Chambers)
Kirtland AFB, NM 87117

1   SAMSO
ATTN: RSSE, MAJ R. Rene
P.O. Box 92960
Los Angeles, CA 90009

DISTRIBUTION LIST

No. of Copies	Organization	No. of Copies	Organization
3	AFTAC ATTN: K. Rosenlof R. McBryde G. Leies Patrick AFB, FL 32925	1	National Academy of Sciences ATTN: Dr. Donald Groves 2101 Constitution Avenue, NW Washington, DC 20418
2	AFML ATTN: G. Schmitt, MAS D. Schmidt Wright-Patterson AFB, OH 45433	1	Aerojet-General Corporation ATTN: Dr. G. Woffinden 11711 South Woodruff Avenue Downey, CA 92041
1	Department of the Interior US Geological Survey ATTN: Dr. D. Roddy 601 East Cedar Avenue Flagstaff, AZ 86001	1	Aerospace Corporation ATTN: Dr. Michael Kausch Bldg 105, Rm 2220 P.O. Box 95085 Los Angeles, CA 90009
2	Energy Research and Development Administration Dept of Military Applications ATTN: R&D Branch Library Branch, G-043 Washington, DC 20545	1	Agbabian Associates ATTN: Dr. J. Malthan 250 N. Nash Street El Segundo, CA 90245
1	Director National Aeronautics and Space Administration ATTN: Code 04.000 Langley Research Center Langley Station Hampton, VA 23365	1	AVCO Government Products Group ATTN: Dr. W. Bade 201 Lowell Street Wilmington, MA 01887
		1	AVCO-Everett Research Lab ATTN: Technical Library 2385 Revere Beach Parkway Everett, MA 02149
1	Director NASA Scientific and Technical Information Facility ATTN: SAK/DL P.O. Box 8757 Baltimore/Washington International Airport, MD 21240	1	Battelle Memorial Institute ATTN: Technical Library 505 King Avenue Columbus, OH 43201
		1	Bell Telephone Laboratories ATTN: Mr. E. Witt Whippany Road Whippany, NJ 07981
2	Los Alamos Scientific Laboratory ATTN: Dr. J. Taylor Technical Library P.O. Box 1663 Los Alamos, NM 87544	1	John A. Blume and Associates ATTN: Dr. John A. Blume Sheraton - Palace Hotel 100 Jessie Street San Francisco, CA 94105

DISTRIBUTION LIST

No. of Copies	Organization	No. of Copies	Organization
1	Calspan Corporation ATTN: Library P.O. Box 235 Buffalo, NY 14221	1	Ion Physics Corporation ATTN: Technical Library South Bedford Street Burlington, MA 01803
1	E. I. duPont de Nemours and Company, Eastern Laboratory Library ATTN: Miss M. Imbrie Givvstown, NJ 08027	3	Kaman Sciences Corporation ATTN: Dr. D. Williams Dr. F. Shelton Dr. D. Sachs 1500 Garden of the Gods Road Colorado Springs, CO 80907
1	Effects Technology, Inc. ATTN: E. Anderson 5383 Holister Avenue Santa Barbara, CA 93105	2	Kaman Avidyne, Div of Kaman Sciences ATTN: Dr. Normal Hobbs Dr. J. Ray Ruetenik 83 - 2nd Avenue, NW Industrial Park Burlington, MA 01803
1	Fairchild Hiller, Republic Aviation Division ATTN: Engr. Library Farmingdale, NY 11735		
1	General Electric Co., TEMPO ATTN: DASIAC 816 State Street, Drawer QQ Santa Barbara, CA 93102	1	KTECH Corporation ATTN: Dr. Donald V. Keller 911 Pennsylvania, NE Albuquerque, NM 87110
3	General Electric Co., TEMPO ATTN: Dr. Craig Hudson Dr. Lynn Kennedy Mr. Gerald L. E. Perry 7800 Marble Avenue NE, Suite 5 Albuquerque, NM 87110	2	Lockheed Missiles and Space Company, Inc. Division of Lockheed Aircraft Corporation ATTN: J. Nickell L. Hearne P.O. Box 504 Sunnyvale, CA 94088
1	H. J. Wiggins Company ATTN: Dr. J. H. Wiggins, Jr. 2516 Via Tejon Palos Verdes Estates, CA 92074	2	Lovelace Foundation ATTN: Dr. D. Richmond Dr. R. Fletcher 4800 Gibson Boulevard, SE Albuquerque, NM 87108
1	Hughes Aircraft Company Systems Development Laboratory ATTN: Dr. A. Puckett Centinela and Teale Streets Culver City, CA 90232	3	Martin Marietta Aerospace, Orlando Division ATTN: A. Ossin H. Sugiuchi C. Washburn P.O. Box 5837 Orlando, FL 32805

41

DISTRIBUTION LIST

No. of Copies	Organization	No. of Copies	Organization
1	Maxwell Laboratories, Inc. ATTN: A. Kolb 9244 Balboa Avenue San Diego, CA 92123	1	Systems, Science and Software, Inc. ATTN: H. E. Read P.O. Box 1620 La Jolla, CA 92037
1	McDonnell Douglas Astronautics Corporation ATTN: Technical Library 5301 Bolsa Avenue Huntington Beach, CA 92647	2	Teledyne - Brown Engineering ATTN: Dr. M. Batel Dr. R. Patrick Research Park Huntsville, AL 35807
1	Philco-Ford Corporation Aeronutronic Division ATTN: L. K. Goodwin Newport Beach, CA 92063	1	Union Carbide Corporation Oak Ridge National Laboratory ATTN: J. Auxier P.O. Box X Oak Ridge, TN 37830
2	Physics International Company ATTN: Document Control F. Sauer 2700 Merced Street San Leandro, CA 94577	1	URS Research Company ATTN: Technical Library 155 Bovet Road San Mateo, CA 94002
1	R&D Associates ATTN: Technical Library P.O. Box 9695 Marina del Rey, CA 90291	1	Denver Research Institute University of Denver ATTN: Mr. John Wisotski P.O. Box 10127 Denver, CO 80210
4	Sandia Laboratories ATTN: Dr. C. Broyles Dr. D. McCloskey Mr. Jack W. Reed Dr. J. Kennedy P.O. Box 5800 Albuquerque, NM 87115	2	IIT Research Institute ATTN: Dr. Robert Denne Technical Library 10 West 35th Street Chicago, IL 60616
1	Science Applications, Inc. ATTN: Dr. T. Stefansky 1261 Birchwood Drive Sunnyvale, CA 94086	1	The John Hopkins University ATTN: Dr. F. D. Bennett Dept of Mechanics and Material Sciences 34th and Charles Streets Baltimore, MD 21218
1	Shock Hydrodynamics, Inc. ATTN: L. Zernow 4710-16 Vineland Avenue North Hollywood, CA 91602	1	Applied Physics Laboratory The Johns Hopkins University Johns Hopkins Road Laurel, MD 20810

DISTRIBUTION LIST

No. of Copies	Organization	No. of Copies	Organization
1	Louisiana State University ATTN: Dr. O. Nance P.O. Box 16006 Baton Rouge, LA 70803	1	Texas Tech. University Department of Civil Engineering ATTN: Mr. Joseph E. Minor Lubbock, TX 79409
1	Massachusetts Institute of Technology Aerophysics Laboratory Cambridge, MA 02139	1	University of Arkansas Department of Physics ATTN: Prof. O. Zinke Fayetteville, AR 72701
1	Northwestern Michigan College ATTN: Prof. D. C. Kennard, Jr. Traverse City, MI 49684	2	University of California Lawrence Livermore Laboratory Technical Information Division ATTN: Technical Library Dr. Donald N. Montan
1	Research Institute of Temple University ATTN: Technical Library Philadelphia, PA 19144		P.O. Box 808 Livermore, CA 94550
1	Southwest Research Institute ATTN: Dr. W. Baker 8500 Culebra Road San Antonio, TX 78206	1	University of Maryland Department of Physics ATTN: Dr. E. Oktay College Park, MD 20742
1	Stevens Institute of Technology Department of Electrical Engineering ATTN: Prof. R. Geldmacher Castle Point Station Hoboken, NJ 07039	1	University of Oklahoma Department of Physics ATTN: Prof. R. Fowler Norman, OK 73069

Aberdeen Proving Ground

1 Syracuse University
Department of Physics
ATTN: Prof. C. Bachman
Syracuse, NY 13201

Marine Corps Ln Ofc
Dir, USAMSAA
ATTN: Dr. J. Sperrazza
Mr. R. Norman, WSD

1 Temple University
Department of Physics
ATTN: Prof. T. Korneff
Philadelphia, PA 19122

43